Optimal fluctuations and tail states of non-Hermitian operators

2001 J. Phys. A: Math. Gen. 34 10805

(http://iopscience.iop.org/0305-4470/34/49/305)

INSTITUTE OF PHYSICS PUBLISHING JOURNAL OF PHYSICS A: MATHEMATICAL AND GENERAL

J. Phys. A: Math. Gen. **34** (2001) 10805–10828 PII: S0305-4470(01)27933-5

Optimal fluctuations and tail states of non-Hermitian operators

F M Marchetti[1,2] **and B D Simons**[1]

[1] Cavendish Laboratory, Madingley Road, Cambridge CB3 OHE, UK
[2] Scuola Normale Superiore, Piazza dei Cavalieri 7, 56126 Pisa, Italy

Received 16 August 2001
Published 30 November 2001
Online at stacks.iop.org/JPhysA/34/10805

Abstract

A statistical field theory is developed to explore the density of states and spatial profile of 'tail states' at the edge of the spectral support of a general class of disordered non-Hermitian operators. These states, which are identified with symmetry broken, instanton field configurations of the theory, are closely related to localized sub-gap states recently identified in disordered superconductors. By focusing separately on the problems of a quantum particle propagating in a random imaginary scalar potential, and a random imaginary vector potential, we discuss the methodology of our approach and the universality of the results. Finally, we address some potential physical applications of our findings.

PACS numbers: 05.45.–a, 02.30.Tb, 11.10.−z, 64.60.–i

(Some figures in this article are in colour only in the electronic version)

1. Introduction

Over recent years the statistical properties of stochastic non-Hermitian operators have come under intense scrutiny [1–19]. Operators of this kind appear in a number of physical applications ranging from random classical dynamics, and statistical physics, to phase breaking and relaxation in quantum dynamics. For example, a straightforward mapping shows the statistical mechanics of a repulsive polymer chain that can be described in terms of the quantum dynamics of a particle subject to a random imaginary scalar potential [20, 21]. Similarly, the statistical mechanics of flux lines in a type-II superconductor pinned by a background of impurities can be described as the quantum evolution of a particle in a disordered environment, subject to an imaginary vector potential [3]. Finally, the diffusion of a classical particle advected by a random velocity field is described by a linear *non-Hermitian* operator, the 'passive scalar' equation [9]. More generally, the dynamics of various classical systems can be expressed in terms of random Fokker–Planck operators (for a review see, e.g. [22, 23]).

Non-Hermitian operators exhibit several qualitatively new phenomena which discriminate their behaviour from those of their random Hermitian counterparts. Firstly, while the eigenvalues of Hermitian operators are real, the spectrum of non-Hermitian operators is

generically complex, bound by some region of support in the complex plane. The second striking distinction concerns the localization properties of the eigenfunctions. It is well established that a weak random impurity potential brings about the localization of all the eigenstates of a Hermitian operator in dimensions of two and lesser [24, 25]. By contrast, a constant imaginary vector potential is sufficient to delocalize the states of the disordered system even in one-dimension! This phenomenon, which was reported and explained by Hatano and Nelson [3], finds extension to higher dimensions [18].

Beginning with the early work on random matrix ensembles [26, 27], a variety of techniques have been developed to study the statistical properties of stochastic non-Hermitian operators [1–19]. Some of the techniques are based on the random matrix theory [1, 2, 6–8, 14, 26, 27], while others involved the development of perturbative schemes, such as the self-consistent Born approximation in the diagrammatic analysis (e.g. [9]). In this paper we are concerned with adapting a third approach which involves the refinement of field theoretic techniques which have proved to be very useful in the description of random Hermitian operators.

Recently, attention has been directed towards the study of 'tail states' which persist at the edge of the spectral support of the non-Hermitian system. Indeed, already there are indications [28–30] that an important role can be played by those parts of the spectrum which are populated by rare states. Now, in stochastic *Hermitian* systems, a small tail of states accumulate below the band edge tightly bound to rare or 'optimal fluctuations' of the random potential [31–34]. These so-called 'Lifshitz tail' states are typically smooth, node-less, localized functions which inhabit regions where the potential is particularly shallow and smooth. By contrast, the character of the complex spectrum in non-Hermitian operators allows the existence of tail states that occupy the entire region which bounds the support of the spectrum.

The difference is not incidental: tail states in the non-Hermitian system can exhibit features characteristic of the quasi-classical states within the bulk spectrum. To emphasize the point, consider the spectrum of, say, a two-dimensional free quantum particle subject to a complex scalar potential, which involves both real *and* imaginary components

$$\hat{H} = \frac{\hat{\boldsymbol{p}}^2}{2m} + \mathrm{i}V(\boldsymbol{r}) + W(\boldsymbol{r}) \tag{1}$$

where $\hat{\boldsymbol{p}} = -\mathrm{i}\hbar\nabla$. If the imaginary potential V is absent, a region of localized tail states accumulate below the band edge ($\epsilon < 0$) due to the optimal configurations of the potential. At energies ϵ greatly in excess of the inverse scattering time $\hbar/\tau$, bulk states are only 'weakly localized' with a localization length ξ_{loc} greatly in excess of scattering mean-free path ℓ and wavelength λ. This is the quasi-classical regime where mechanisms of quantum interference strongly affect the spectral and transport properties of the system [24, 25].

In this background, let us now suppose that a small imaginary component of the potential is restored. Being non-Hermitian, the eigenvalues migrate into the complex plane occupying a finite region of support centred on the real axis (see figure 1). At the level of the mean-field analysis (detailed below), complex eigenvalues are confined to a sharp region of support in the complex plane. However, as with Lifshitz states, optimal fluctuations of the random potential(s) generate states which lie outside the region of support (see figure 1). What is the nature of these states? Are they localized and, if so, over what length scale? Here, in contrast to the Hermitian system, tail states must accommodate fast fluctuations of the wavefunction at the scale of the wavelength of the Hermitian system.

To our knowledge, the problem of tail states in the non-Hermitian system was first considered in a recent work by Izyumov and Simons [16]. Refining an approach developed in [33, 34] to explore tail states in Hermitian systems, the authors introduced a non-perturbative scheme to investigate states at the edge of the support in non-Hermitian systems. This

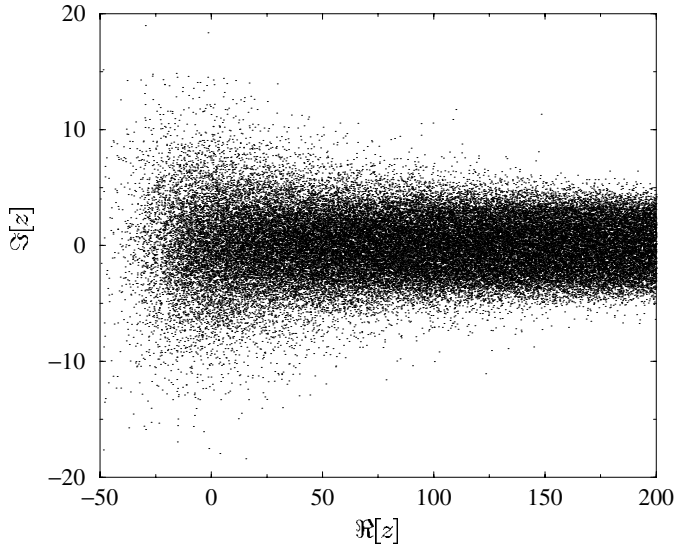

Figure 1. Complex eigenvalue spectrum for several realizations of the random non-Hermitian Hamiltonian (1), where the potentials V and W are both drawn from a Gaussian δ-correlated random impurity distribution. Here we have included a lattice of 29×29 $\boldsymbol{q}$-points in the momentum space.

instanton technique revealed the existence of tail states at the edge which are localized on a length scale greatly in excess of the wavelength—tail states in the non-Hermitian system are quasi-classical in nature. Building on the work of Efetov [35], the aim of the present paper is to develop a supersymmetric field theory to explore the spatial profile of the states in the tail region, and to determine the complex density of states (DoS) in the vicinity of the band edge. In doing so, we will reveal a close correspondence between tail states in the non-Hermitian problem and sub-gap states in the weakly disordered superconductors. Moreover, constraints within the present scheme reveals the universal character of tail states in the non-Hermitian system showing that, after a suitable rescaling, the profile of the DoS tail depends only on dimensionality and separation from the support. In particular, in contrast to Lifshitz states in the Hermitian system, properties of the tail states are universal, independent of the nature of the random distribution.

To illustrate the generality of our approach we will consider two examples which, according to the classification scheme defined below, belong to different fundamental symmetry. Firstly, following our discussion above, we will investigate the properties of tail states in a quantum system involving the propagation of a particle in a random *scalar* potential involving both real *and* imaginary components (1). Secondly, we will investigate the nature of tails states in a quantum system where the particle is subject to a random real scalar potential and a random imaginary *vector* potential

$$\hat{H} = \frac{[\hat{\boldsymbol{p}} + \mathrm{i}\boldsymbol{h}(\boldsymbol{r})]^2}{2m} + W(\boldsymbol{r}). \tag{2}$$

As well as in the Hatano–Nelson system [3], $\boldsymbol{h} = \text{const}$, (2) has been studied in the context of random classical dynamics involving classical diffusion in the background of a quenched random velocity field. Identifying $1/2m$ with the classical diffusion constant D, and $\boldsymbol{h}/2m$ with

a random velocity field $\boldsymbol{v}$, a redefinition of the random potential $W(\boldsymbol{r})$ obtains the classical operator

$$\hat{H} = -D\nabla^2 + (\nabla \cdot \boldsymbol{v}) + \boldsymbol{v} \cdot \nabla + \bar{W}(\boldsymbol{r}).$$

In the quasi-classical approximation, (i.e. setting z as the complex energy, where $\tau\Re[z] \gg \hbar$) our goal will be to show that the long-range, low-energy properties of the random systems are described by a supersymmetric non-linear σ-model. At the level of the mean-field, the spectrum of both non-Hermitian operators is seen bound to a region of support inside the complex plane. By taking into account the non-perturbative symmetry-breaking instanton field configurations of the action, we will reveal the existence of tail states which extend beyond the region of support predicted by the mean-field. We will determine the localization properties and profile of the DoS revealing an intrinsic universality of the present scheme.

The paper is organized as follows: after introducing a general scheme to classify linear non-Hermitian operators on the basis of their fundamental symmetries, in section 2 we formulate a statistical field theory to describe the spectral properties of the random imaginary scalar potential Hamiltonian. Within this approach, we show that the large scale properties of the spectral support are determined by the saddle-point or mean-field properties of the theory. Motivated by a parallel description of the disordered superconducting system, in section 2.3 we show that optimal fluctuations of the random impurity potential induce localized tail states which extend beyond the region of support. Within this approach, we determine analytical expressions for the spatial extent of the localized states in the tail region, and determine the scaling of the complex DoS as a function of energy. Generalizing the scheme for the consideration of the imaginary vector potential Hamiltonian in section 3, we emphasize the universality of the present scheme. Results from both sections are compared with numerical simulations. Finally, in section 4 we conclude our discussion.

2. Field theory of non-Hermitian operators

The aim of this section is to prepare a statistical field theory of the weakly disordered non-Hermitian system. To be concrete, in the first instance, we will focus on the problem of the imaginary scalar potential (1). Later, we will see that the field theoretic scheme is easily modified to accommodate the constant vector potential perturbation. However, before embarking on this program, it is useful to first contrast the general properties of complex linear non-Hermitian operators with those of their Hermitian counterparts. Along with helping to clarify the idiosyncrasies of the non-Hermitian system, we will expose a general scheme in which non-Hermitian operators can be classified according to their fundamental symmetries.

2.1. Background: symmetry classification

A general non-Hermitian operator $\hat{H}$ is specified by left and right eigenfunctions

$$\hat{H}|R_i\rangle = z_i|R_i\rangle \qquad \langle L_i|\hat{H} = \langle L_i|z_i$$

where $\{z_i\}$ denotes the set of complex eigenvalue. Although it is not a generic feature of non-Hermitian operators, we will rely throughout on the assumption that the eigenfunctions form a complete basis set. This is the case if there are no repeated eigenvalues, which will be true for a generic random operator such as those studied here. Furthermore, we will take the eigenstates to be orthonormal,

$$\langle L_i|R_j\rangle = \delta_{ij} \qquad \sum_i |R_i\rangle\langle L_i| = \mathbb{I}. \tag{3}$$

Now as with Hermitian operators, spectral (and localization) properties of the non-Hermitian Hamiltonian can be expressed through the complex Green function

$$\hat{g}(z) = \frac{1}{z - \hat{H}}$$

where $z = x + \mathrm{i}y$ denotes the complex argument. Inserting the resolution of identity (3), one obtains the spectral decomposition,

$$\hat{g}(z) = \sum_i |R_i\rangle \frac{1}{z - z_i} \langle L_i|. \tag{4}$$

Using the analytical properties of the resolvent, it is straightforward to show that the density of the complex eigenvalues

$$\nu(z) = \frac{1}{L^d} \operatorname{tr} \delta(z - \hat{H}) = \frac{1}{\pi L^d} \lim_{\eta \to 0} \sum_i \frac{\eta^2}{(|z - z_i|^2 + \eta^2)^2}$$

is expressible in terms of the complex Green function through the identity (4)

$$\nu(z) = \frac{1}{\pi L^d} \partial_{z^*} \operatorname{tr} \hat{g}(z).$$

The complex Green function $\hat{g}(z)$ is, therefore, a non-analytic function everywhere in the complex z-plane in which the corresponding eigenvalues density is non-vanishing.

Previous studies have shown that techniques based on standard diagrammatic perturbation theory account only for contributions to $\hat{g}(z)$ which are *analytic* in z [1]. To account for all contributions, it is convenient to follow the now standard route [8, 9, 27] of expressing the Green function through an auxiliary Hamiltonian which is explicitly Hermitian. This is achieved by constructing a matrix Hamiltonian, $\hat{\mathcal{H}}$, with the following 2×2 block structure

$$\hat{\mathcal{H}} = \begin{pmatrix} 0 & \hat{H} - z \\ \hat{H}^\dagger - z^* & 0 \end{pmatrix}.$$

In this representation, the Green function of the non-Hermitian operator is expressed as the off-diagonal element of the matrix Green function [9],

$$\hat{g}(z) = \lim_{\eta \to 0} \hat{G}_{21}(\eta, z)$$

where $\hat{G}(\eta, z) = (\mathrm{i}\eta - \hat{\mathcal{H}})^{-1}$.

This 'method of Hermitization' affords a convenient way of classifying the symmetries of a non-Hermitian Hamiltonian according to the fundamental symmetries of its Hermitian counterpart. The utility of this classification will become manifest presently in the construction of the statistical field theory of the non-Hermitian system. As an example, let us consider the Hamiltonian involving an imaginary scalar potential (1). Applied to this problem, the Hermitization procedure leads to the matrix Hamiltonian

$$\hat{\mathcal{H}} = \left(\hat{\xi}_{\hat{\boldsymbol{p}}} - x + W\right) \sigma_1 + (y - V)\, \sigma_2$$

where the Pauli matrices σ_i act in the 2×2 sub-space, and $\hat{\xi}_{\hat{\boldsymbol{p}}} = \hat{\boldsymbol{p}}^2/2m$.

In fact, the matrix structure of $\hat{\mathcal{H}}$ bears much in common with the Gor'kov or Bogoliubov-de Gennes quasi-particle Hamiltonian of a weakly disordered superconductor [15]. To foster this analogy, let us implement the canonical transformation

$$\hat{\mathcal{H}} \mapsto \hat{\mathcal{H}}_\Gamma = \Gamma^{-1} \hat{\mathcal{H}} \Gamma = \left(\hat{\xi}_{\hat{\boldsymbol{p}}} - x + W\right) \sigma_3 + (y - V)\, \sigma_2 \tag{5}$$

where $\Gamma = \exp[-\mathrm{i}\pi\sigma_2/4]$. Associating the matrix structure with a 'particle/hole' space, the operator $\hat{\mathcal{H}}_\Gamma$ can be identified as a Gor'kov Hamiltonian for a disordered superconductor.

Here x plays the role of the chemical potential, while $\hat{\zeta}_{\hat{p}} + W$ denotes the bare Hamiltonian and $(y - V)$ represents the (in this case real, random) order parameter. However, taking the analogy further, the energy argument in the Gor'kov Green function corresponds, in this case, to the infinitesimal $i\eta$ of the matrix Green function $\hat{G}_\Gamma^{-1}(\eta, z)$—evidently, we are interested in the zero-energy quasi-particle states of the disordered, time-reversal invariant superconductor with a random real order parameter.

In its Hermitian form, the above Hamiltonian can be classified according to its fundamental symmetries. According to the classification introduced by Zirnbauer [36], the matrix construction places a general non-Hermitian Hamiltonian in the chiral unitary symmetry class denoted AIII[3], a general element of which has the form

$$\begin{pmatrix} 0 & Z \\ Z^\dagger & 0 \end{pmatrix}$$

where Z is an arbitrary complex matrix. However, within this group, there are four subclasses of higher symmetry: class CI (the time-reversal invariant superconductor) where matrices Z are complex symmetric; class BDI (chiral orthogonal) where the elements of Z are arbitrary and real; class CII where Z has an underlying symplectic structure; and class DIII where Z is complex antisymmetric. As will be clear from the forthcoming analysis, the statistical field theory describing the non-Hermitian spectral properties has soft modes associated with each universality class. From our discussion above, the imaginary scalar potential is accommodated in the symmetry class CI.

As the second example, let us consider the non-Hermitian Hamiltonian (2) involving the random imaginary vector potential. In this case, the Hermitization procedure leads to the matrix Hamiltonian

$$\hat{\mathcal{H}}_\Gamma = \left(\frac{\hat{\boldsymbol{p}}^2 - \boldsymbol{h}^2}{2m} + W - x \right) \sigma_3 + \left(y - \frac{\hat{\boldsymbol{p}} \cdot \boldsymbol{h} + \boldsymbol{h} \cdot \hat{\boldsymbol{p}}}{2m} \right) \sigma_2. \tag{6}$$

As a result, we find that the system belongs to a different class depending on the value of the imaginary component of the energy argument y. Along the real axis (i.e. for $y = 0$) $\hat{\mathcal{H}}$ is real and therefore belongs to the symmetry class BDI. Away from the real axis the Hamiltonian becomes complex and the symmetry is lowered to class AIII. Later we will discuss the physical manifestations of the discrete symmetries in the two limits.

2.2. Generating functional

With this background, let us now turn to the construction of a field theory to describe statistical correlations of the non-Hermitian model. Motivated by the correspondence outlined above, the analysis will parallel previous investigations of the weakly disordered superconductor [37–39]. The starting point is the generating functional for the single-particle Green function. Adopting the convention $\hbar = c = 1$ throughout, the latter is expressed as a field integral involving two independent four-component supervector fields $\psi(\boldsymbol{r})$ and $\bar{\psi}(\boldsymbol{r})$ with elements having both commuting/anti-commuting and 'particle/hole' indices:

$$\mathcal{Z}[j] = \int D(\bar{\psi}, \psi) \exp\left[\mathrm{i} \int \mathrm{d}\boldsymbol{r}\ \bar{\psi}(\mathrm{i}\eta - \hat{\mathcal{H}})\psi + \int \mathrm{d}\boldsymbol{r}(\bar{\psi} j + \bar{j}\psi) \right].$$

[3] The notation adopted by Zirnbauer is motivated by that introduced by Cartan to classify the 10 + 1 symmetric spaces.

Elements of the Green function can be generated from the source terms $j(\boldsymbol{r})$ and $\bar{j}(\boldsymbol{r})$. For example, from the generating function one can obtain the DoS according to the identity

$$\nu(z) = \frac{\mathrm{i}}{\pi}\partial_{z^*}\lim_{\eta\to 0}\int \frac{\mathrm{d}\boldsymbol{r}}{L^d}\,\frac{\delta^2}{\delta \bar{j}_2^{\mathrm{B}}(\boldsymbol{r})\delta j_1^{\mathrm{B}}(r)}Z[j]\bigg|_{j=0}. \tag{7}$$

To be concrete, let us first consider the properties of the Hamiltonian involving the imaginary scalar potential. To exploit the analogy with the superconducting system, it is again convenient to implement the gauge transformation $\psi \mapsto \Gamma\psi$ whereupon the generating functional assumes the form

$$\mathcal{Z}[0] = \int D(\bar{\psi},\psi)\exp\left[\mathrm{i}\int \mathrm{d}\boldsymbol{r}\;\bar{\psi}(\boldsymbol{r})\left(\mathrm{i}\eta - \hat{\mathcal{H}}_\Gamma\right)\psi(\boldsymbol{r})\right] \tag{8}$$

where $\hat{\mathcal{H}}_\Gamma$ is defined above (5). Now, as with the superconductor, the matrix Hamiltonian (6) satisfies the particle/hole or 'charge-conjugation' (CC) symmetry

$$-\sigma_2\hat{\mathcal{H}}_\Gamma^{\mathsf{T}}\sigma_2 = \hat{\mathcal{H}}_\Gamma.$$

The latter is responsible for quantum interference effects which modify the long-range or low-energy properties of the average Green function. To accommodate these effects it is convenient to double the field space

$$\begin{aligned}2\bar{\psi}(\mathrm{i}\eta - \hat{\mathcal{H}}_\Gamma)\psi &= \bar{\psi}(\mathrm{i}\eta - \hat{\mathcal{H}}_\Gamma)\psi + \psi^{\mathsf{T}}(\mathrm{i}\eta - \hat{\mathcal{H}}_\Gamma^{\mathsf{T}})\bar{\psi}^{\mathsf{T}}\\ &= \bar{\psi}\left(\mathrm{i}\eta - \hat{\mathcal{H}}_\Gamma\right)\psi + \psi^{\mathsf{T}}(\mathrm{i}\eta + \sigma_2\hat{\mathcal{H}}_\Gamma\sigma_2)\bar{\psi}^{\mathsf{T}} = 2\bar{\Psi}(\mathrm{i}\eta\sigma_3^{\mathrm{cc}} - \hat{\mathcal{H}}_\Gamma)\Psi\end{aligned}$$

where, defining the Pauli matrix σ_3^{cc} which operates in the charge-conjugation (CC) space,

$$\Psi = \frac{1}{\sqrt{2}}\begin{pmatrix}\psi\\ \sigma_2\bar{\psi}^{\mathsf{T}}\end{pmatrix}_{\mathrm{cc}} \qquad \bar{\Psi} = \frac{1}{\sqrt{2}}\left(\bar{\psi} - \psi^{\mathsf{T}}\sigma_2\right)_{\mathrm{cc}}.$$

As a result, the generating functional takes the form

$$\mathcal{Z}[0] = \int D(\bar{\Psi},\Psi)\exp\left\{\mathrm{i}\int \mathrm{d}\boldsymbol{r}\;\bar{\Psi}(\boldsymbol{r})\left[\mathrm{i}\eta\sigma_3^{\mathrm{cc}} + \left(x - \hat{\zeta}_{\hat{p}} - W\right)\sigma_3 - (y - V)\,\sigma_2\right]\Psi(\boldsymbol{r})\right\}.$$

With this definition, the fields Ψ and $\bar{\Psi}$ are not independent but obey the symmetry relations

$$\Psi = \sigma_2\gamma\bar{\Psi}^{\mathsf{T}} \qquad \bar{\Psi} = -\Psi^{\mathsf{T}}\sigma_2\gamma^{\mathsf{T}} \tag{9}$$

with $\gamma = E_{\mathrm{BB}}\otimes\sigma_1^{\mathrm{CC}} - \mathrm{i}E_{\mathrm{FF}}\otimes\sigma_2^{\mathrm{CC}}$, where $E_{\mathrm{BB}} = \mathrm{diag}(1,0)_{\mathrm{BF}}$ and $E_{\mathrm{FF}} = \mathrm{diag}(0,1)_{\mathrm{BF}}$ are the projectors on the boson–boson and fermion–fermion sectors, respectively. This completes the construction of the generating functional as a functional field integral. To make further progress, we can draw on the intuition afforded by existing studies of the superconducting system.

2.2.1. Disorder averaging. As a first step towards the construction of an effective low-energy theory, it is necessary to subject the generating functional to an ensemble average over the random impurity distribution. For this purpose we will take both the real and imaginary components of the random scalar potential to be Gaussian δ-correlated with zero mean, and correlation

$$\langle W(\boldsymbol{r}_1)W(\boldsymbol{r}_2)\rangle_W = \frac{1}{2\pi\nu\tau}\delta^d(\boldsymbol{r}_1 - \boldsymbol{r}_2) \qquad \langle V(\boldsymbol{r}_1)V(\boldsymbol{r}_2)\rangle_V = \frac{1}{2\pi\nu\tau_n}\delta^d(\boldsymbol{r}_1 - \boldsymbol{r}_2) \tag{10}$$

where $\nu \equiv (\Delta L^d)^{-1} \sim m(2mx)^{(d-2)/2}$ represents the unperturbed DoS of the Hermitian Hamiltonian $\hat{\zeta}_{\hat{p}}$ at energy x, while τ and τ_n denote, respectively, the mean scattering time of the real and imaginary components of the potential. In the following, we will suppose that the imaginary component of the scattering potential is weak, i.e. $\tau_n \gg \tau$.

The ensemble averaging over the real random scalar potential $W(\boldsymbol{r})$ induces an interaction of the fields which can be decoupled by the introduction of an 8×8 component Hubbard–Stratonovich field Q,

$$\left\langle \exp\left[-\mathrm{i}\int \mathrm{d}\boldsymbol{r}\ \bar{\Psi} W \sigma_3 \Psi\right]\right\rangle_W = \int DQ \exp\left[\int \mathrm{d}\boldsymbol{r}\left(\frac{\pi\nu}{8\tau}\mathrm{str}\, Q^2 - \frac{1}{2\tau}\bar{\Psi} Q \sigma_3 \Psi\right)\right].$$

Transforming the fields according to the symmetry (9), one finds that the supermatrix fields, $Q(\boldsymbol{r})$, must be subjected to the constraint

$$Q = \sigma_1 \gamma Q^{\mathsf{T}} \gamma^{\mathsf{T}} \sigma_1. \tag{11}$$

Similarly, the interaction of the fields induced by the ensemble average over the random imaginary scalar potential $V(\boldsymbol{r})$ can be decoupled by an 8×8 component Hubbard–Stratonovich field $P(\boldsymbol{r})$, satisfying the symmetry constraint, $P = \gamma P^{\mathsf{T}} \gamma^{\mathsf{T}}$:

$$\left\langle \exp\left[\mathrm{i}\int \mathrm{d}\boldsymbol{r}\ \bar{\Psi} V \sigma_2 \Psi\right]\right\rangle_V = \int DP \exp\left[\int \mathrm{d}\boldsymbol{r}\left(\frac{\pi\nu}{8\tau_n}\mathrm{str}\, P^2 - \frac{1}{2\tau_n}\bar{\Psi} P \sigma_2 \Psi\right)\right].$$

Finally, an integration over the fields Ψ obtains

$$\langle \mathcal{Z}[0]\rangle_{W,V} = \int DQ \int DP \exp\left\{\frac{\pi\nu}{8}\int \mathrm{d}\boldsymbol{r}\ \mathrm{str}\left(\frac{Q^2}{\tau} + \frac{P^2}{\tau_n}\right) - \frac{1}{2}\int \mathrm{d}\boldsymbol{r}\ \mathrm{str}\langle \boldsymbol{r}|\ln \hat{\mathcal{G}}^{-1}|\boldsymbol{r}\rangle\right\}$$

where

$$\hat{\mathcal{G}}^{-1} = \mathrm{i}\eta\sigma_3 \otimes \sigma_3^{\mathrm{CC}} + x - \hat{\zeta}_{\hat{p}} - \mathrm{i}y\sigma_1 + \frac{\mathrm{i}}{2\tau}Q - \frac{1}{2\tau_n}P\sigma_1$$

represents the supermatrix Green function. Further progress in this case is possible only within the saddle-point approximation. Following [37], in the quasi-classical approximation $x \gg 1/\tau \gg [1/\tau_n, y]$, it is convenient to implement a two-level procedure in which we first formulate an 'intermediate energy-scale' action in which the terms in y and $1/\tau_n$ are treated as small symmetry-breaking sources. Later, the influence of V (through P) on the complex DoS can be explored within a stationary analysis of this reduced action.

2.2.2. Intermediate energy-scale action. Neglecting the terms in y and P, a variation of the action with respect to Q obtains the saddle-point equation

$$Q(\boldsymbol{r}) = \frac{\mathrm{i}}{\pi\nu}\mathcal{G}_0(\boldsymbol{r},\boldsymbol{r}) \qquad \hat{\mathcal{G}}_0^{-1} = \mathrm{i}\eta\sigma_3^{\mathrm{CC}} \otimes \sigma_3 + x - \hat{\zeta}_{\hat{p}} + \frac{\mathrm{i}}{2\tau}Q.$$

In the quasi-classical limit, $x\tau \gg 1$, taking Q to be homogeneous in space, this equation can be solved in the pole approximation with $Q = \pm 1$. Taking into account the analytical properties of the average Green function, we identify the solution $Q_{\mathrm{sp}} = \sigma_3 \otimes \sigma_3^{\mathrm{CC}}$. However, in the limit $\eta \to 0$, the saddle-point solution is not unique, but expands to span a degenerate manifold of solutions generated by the homogeneous pseudo-unitary transformations $Q_{\mathrm{sp}} = T\sigma_3 \otimes \sigma_3^{\mathrm{CC}} T^{-1}$ compatible with the symmetry of Q (11).

Fluctuations around the saddle-point can be classified into longitudinal and transverse modes according to whether they violate the non-linear constraint $Q^2(\boldsymbol{r}) = \mathbb{I}$ or not. In the quasi-classical limit, the longitudinal fluctuations are rendered massive and do not contribute to the low-energy properties of the generating functional. On the other hand, transverse fluctuations of the fields become soft and must be accommodated. Taking into account soft fluctuations $Q(\boldsymbol{r}) = T(\boldsymbol{r})\sigma_3 \otimes \sigma_3^{\mathrm{CC}} T^{-1}(\boldsymbol{r})$, and restoring the perturbations y and P, a gradient expansion of the action obtains the average generating functional

$$\langle \mathcal{Z}[0]\rangle_{W,V} = \int_{Q^2=\mathbb{I}} DQ \int DP \exp\left\{\frac{\pi\nu}{8\tau_n}\int \mathrm{d}\boldsymbol{r}\ \mathrm{str}\, P^2\right\}$$
$$\times \exp\left\{\frac{\pi\nu}{8}\int \mathrm{d}\boldsymbol{r}\ \mathrm{str}\left[D(\nabla Q)^2 + 4\mathrm{i}\left(\mathrm{i}\eta\sigma_3 \otimes \sigma_3^{\mathrm{CC}} - \mathrm{i}y\sigma_1 - \frac{P}{2\tau_n}\sigma_1\right)Q\right]\right\}$$

where $D = v_F^2\tau/d$ is the diffusion constant. Here we have neglected the higher order terms in $y\tau$ and τ/τ_n. In the same approximation $y\tau \ll 1$, the supermatrix Green function takes the form [35]

$$\mathcal{G}_0(\boldsymbol{r},\boldsymbol{r}') = -\mathrm{i}\pi\nu f_d(|\boldsymbol{r}-\boldsymbol{r}'|)\,Q\left(\frac{\boldsymbol{r}+\boldsymbol{r}'}{2}\right)$$

where $f_d(r) = \Gamma(d/2)[2/k_F r]^{d/2-1}J_{d/2-1}(k_F r)\exp[-r/2\ell]$ is the Friedel function, and $k_F = \sqrt{2mx}$.

Finally, integrating over the supermatrices P, we obtain the average generating functional

$$\langle\mathcal{Z}[0]\rangle_{W,V} = \int_{Q^2=\mathbb{I}} DQ\exp\{-S[Q]\}$$

where

$$S[Q] = -\frac{\pi\nu}{8}\int \mathrm{d}\boldsymbol{r}\ \mathrm{str}\left[D(\nabla Q)^2 - 4\left(\eta\sigma_3\otimes\sigma_3^{\mathrm{CC}} - y\sigma_1\right)Q + \frac{1}{\tau_n}(\sigma_1 Q)^2\right]. \tag{12}$$

This completes the construction of the intermediate energy-scale action for the non-Hermitian system. Returning to the analogy with the superconductor, we note that the form of the action (12) coincides with that of a disordered superconductor subject to a random real-order parameter with an average magnitude y and variance set by $1/\tau_n$. To investigate the influence of the imaginary potential on the complex DoS, it is necessary to subject this action to a further stationary analysis and obtain the low-energy action.

2.2.3. Low-energy scale action. Although the soft-mode action (12) is stabilized by the quasi-classical parameter $x\tau$, the terms in y and $1/\tau_n$ render the majority of field fluctuations massive. To obtain the low-energy saddle-point, let us again vary the action with respect to Q subject to the non-linear constraint, $Q^2 = \mathbb{I}$:

$$D\nabla(Q\nabla Q) - \left[\eta\sigma_3\otimes\sigma_3^{\mathrm{CC}} - y\sigma_1,\, Q\right] + \frac{1}{2\tau_n}[\sigma_1 Q\sigma_1,\, Q] = 0.$$

Applying the ansatz $Q = \cos\hat{\theta}\sigma_3\otimes\sigma_3^{\mathrm{CC}} + \sin\hat{\theta}\sigma_1$, where $\hat{\theta} = \mathrm{diag}(\mathrm{i}\theta_{\mathrm{BB}}, \theta_{\mathrm{FF}})_{\mathrm{B,F}}$, the saddle-point equation assumes the form

$$D\nabla^2\hat{\theta} - 2[\eta\sin\hat{\theta} + y\cos\hat{\theta}] - \frac{1}{\tau_n}\sin 2\hat{\theta} = 0 \tag{13}$$

a result reminiscent of the Abrikosov–Gor'kov mean-field equation of the disordered superconductor subject to a pair-breaking perturbation [40]. Taking the solution to be symmetric and homogeneous in space, one obtains

$$\mathrm{i}\theta_{\mathrm{BB}} = \theta_{\mathrm{FF}} = \theta_{\mathrm{MF}} = \begin{cases} -\arcsin(y\tau_n) & |y|\tau_n < 1 \\ -\frac{\pi}{2}\mathrm{sign}(y) & |y|\tau_n \geqslant 1. \end{cases} \tag{14}$$

Once again, as $\eta \to 0$, this solution is not unique but expands to span an entire manifold parameterized by transformations $Q = TQ_{\mathrm{MF}}T^{-1}$, where $[T,\sigma_1] = 0$ and $T = \gamma(T^{-1})^{\mathsf{T}}\gamma^{\mathsf{T}}$ which represent the soft fluctuations corresponding to the time-reversal invariant superconductor symmetry class CI. Substituted back into the action, these fluctuations are described by the corresponding low-energy action [15]

$$S_{\mathrm{eff}}[\bar{Q}] = -\frac{\pi\nu}{8}\int \mathrm{d}\boldsymbol{r}\ D\left(1 - y^2\tau_n^2\right)\mathrm{str}(\nabla\bar{Q})^2$$

where $\bar{Q} = T\sigma_3\otimes\sigma_3^{\mathrm{CC}}T^{-1}$. This completes our construction of the field theory describing spectral correlations in the disordered non-Hermitian system. In the following section we will use these results to explore the support of the complex DoS.

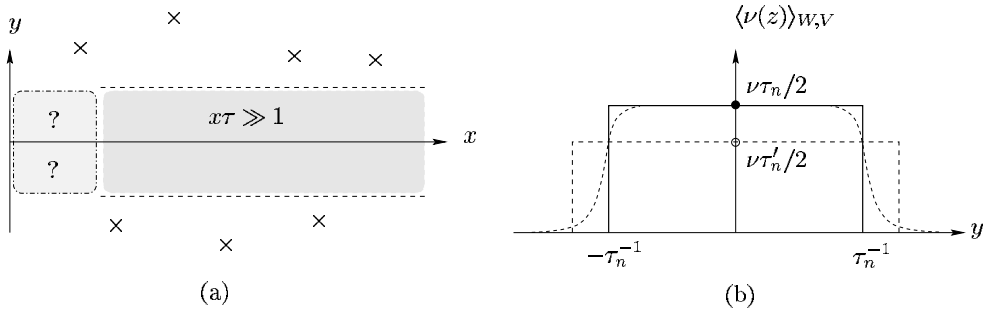

Figure 2. Complex DoS in the quasi-classical limit $x\tau \gg 1$ for the two-dimensional scalar potential problem. (*a*) In the mean-field approximation, the DoS is equal to $\nu\tau_n/2$ inside the region $|y|\tau_n \leqslant 1$ of the complex plane $z = x + \mathrm{i}y$ and zero outside. (*b*) $\langle\nu(z)\rangle_{W,V}$ versus y for a fixed x and for two values of the scattering time, $\tau_n > \tau_n'$: while in the mean-field approximation the DoS shows sharp edges, rare realizations of the random potential give rise to tail states (section 2.3).

2.3. Complex density of states

Making use of equation (7), the complex DoS is obtained from the generating function as

$$\langle\nu(z,\boldsymbol{r})\rangle_{W,V} = -\frac{\mathrm{i}}{4}\nu\partial_{z^*}\lim_{\eta\to 0}\left\langle \mathrm{str}\left[(\mathbb{I}-\sigma_1)\otimes E_{\mathrm{CC}}^{11}\otimes\sigma_3^{\mathrm{BF}}Q(\boldsymbol{r})\right]\right\rangle_Q \tag{15}$$

where $\langle\cdots\rangle_Q = \int_{Q^2=\mathbb{I}} DQ\cdots \mathrm{e}^{-S[Q]}$ where $S[Q]$ represents the intermediate energy-scale action (12). In the homogeneous saddle-point (i.e. mean-field) approximation (14), the corresponding DoS takes the form

$$\langle\nu(z)\rangle_{W,V} = \mathrm{i}\nu\partial_{z^*}\lim_{\eta\to 0}\sin\theta_{\mathrm{MF}} = \begin{cases} \frac{\nu\tau_n}{2} & |y|\tau_n < 1 \\ 0 & |y|\tau_n \geqslant 1. \end{cases} \tag{16}$$

As expected, at the level of the mean-field, the field theory predicts a migration of the DoS off the real line and into the complex plane. The density of complex eigenvalues is constant over the region of support set by the effective scattering rate of the non-Hermitian potential. Reassuringly, the expression for the DoS satisfies the sum rule $\int \mathrm{d}y\langle\nu(z)\rangle_{W,V} = \nu$. In the two-dimensional case, the result is illustrated qualitatively in figure 2. As the scattering time τ_n does not depend on the real part of the energy x, the width of the mean-field spectrum boundary is constant.

To complete the analysis, it is necessary to take into account the fluctuations of the fields around the saddle-point. As discussed above, these fluctuations divide into a set which is massive (on the scale of y) and a massless set. Interestingly, one finds that the latter commute with the source and do not contribute to the DoS!

Indeed, the general profile of the support is born out by numerical simulation. Figure 1 shows the amalgamation of data for the two-dimensional random system generated from 100 realizations of the complex random scalar potential Hamiltonian. However, instead of a sharp cut-off in the support, the data clearly indicate a soft edge with eigenvalues occupying the region outside the mean-field prediction (16). How can this observation be reconciled with the results of the field theory? Surprisingly, taking into account massive fluctuations of the action perturbatively, the mean-field prediction remains intact. In fact, the tail states that decorate the edge of the support are generated by optimal fluctuations of the *real* random impurity potential and are reflected in *non-perturbative* instanton configurations of the action.

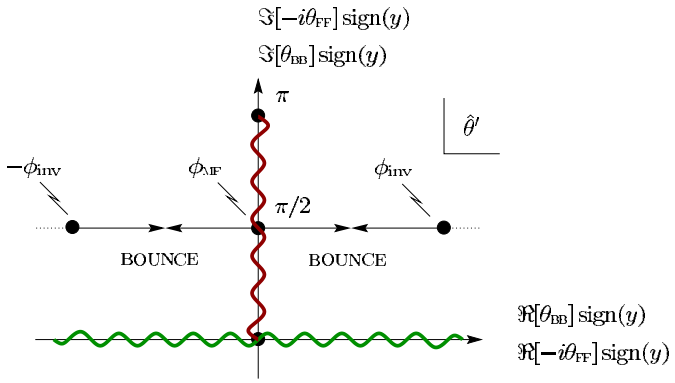

Figure 3. Integration contours for boson–boson and fermion–fermion fields in the complex plane $\hat{\theta}' = -\mathrm{i}\hat{\theta}\ \mathrm{sign}(y)$. The two degenerate bounce solutions are qualitatively shown, together with the mean-field starting point $\phi_{\rm MF}$ and the inversion point $\phi_{\rm inv}$.

2.4. Tail states and instantons

To identify corrections to the mean-field DoS (16), we can draw on the intuition afforded by recent studies of sub-gap state formation due to optimal fluctuations in the superconducting system [41]. While the homogeneous solution of the mean-field equation gives rise to a hard edge of the DoS support, we will see that inhomogeneous symmetry-broken field configurations reflect the influence of rare realizations or 'optimal fluctuations' of the random scalar potentials which soften the edge (figure 2). Here, for simplicity, let us focus on the quasi one-dimensional case, generalizing the discussion to the d-dimensional system in section 2.4.2.

2.4.1. Quasi one-dimensional geometry. To explore the influence of inhomogeneous field configurations of the action, let us revisit the mean-field equation of motion (13). Operationally, it is convenient to not deal with the saddle-point equation (13) itself, but rather its first integral, $D(\nabla\hat{\theta})^2 - yV(\hat{\theta}) = \text{const}$, where

$$V(\hat{\theta}) = -4\left[\frac{\eta}{y}\cos\hat{\theta} - \sin\hat{\theta}\right] - \frac{1}{y\tau_n}\cos 2\hat{\theta}$$

denotes the effective complex 'potential'.

To identify the inhomogeneous instanton solution, let us first note that outside the region of support, $|y|\tau_n \geqslant 1$, the homogeneous mean-field solution takes the form $\theta_{\rm MF} = -\pi/2\,\mathrm{sign}(y)$. Taking into account the condition that the solution should coincide with $\theta_{\rm MF}$ at infinity, one can identify a 'bounce' solution parameterized by $\theta = [-\pi/2 + \mathrm{i}\phi]\mathrm{sign}(y)$, with ϕ real, involving the *real* potential $V_{\rm R}(\phi) \equiv V([-\pi/2 + \mathrm{i}\phi]\mathrm{sign}(y))$ with endpoint $\phi_{\rm inv}$ such that $V_{\rm R}(\phi_{\rm inv}) = V_{\rm R}(\phi_{\rm MF})$.

Now integration over the angles $\hat{\theta}$ is constrained to certain contours [35]. Is the bounce solution accessible to both? As usual, the contour of integration over the boson–boson field $\theta_{\rm BB}$ includes the entire real axis, while for the fermion–fermion field $\mathrm{i}\theta_{\rm FF}$ runs along the imaginary axis from 0 to $\mathrm{i}\pi$. With a smooth deformation of the integration contours, the mean-field saddle-point is accessible to both the angles $\hat{\theta}$ [37, 38]. By contrast, the particular bounce solution *and* the mean-field solution can be reached simultaneously by a smooth deformation of the integration contour *only* for the boson–boson field $\theta_{\rm BB}$ (see figure 3). The particular bounce solution breaks the supersymmetry.

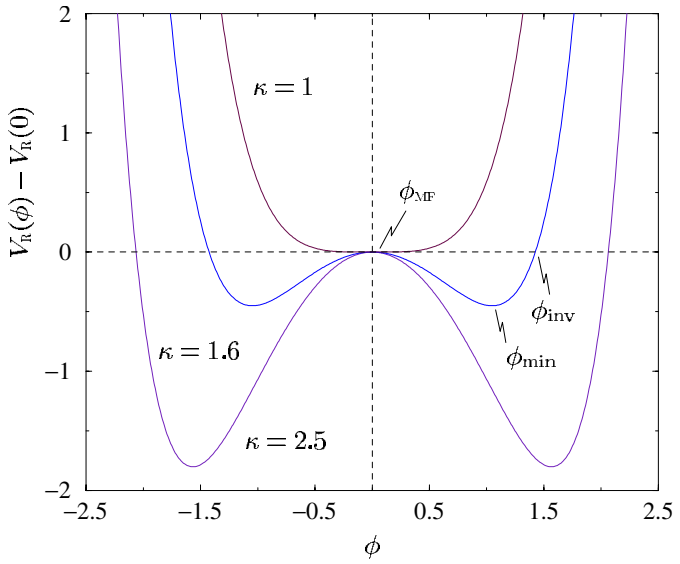

Figure 4. Rescaled potential $V_{\rm R}(\phi) - V_{\rm R}(0)$ versus the variable ϕ for $\kappa = 2.5$, $\kappa = 1.6$ and $\kappa = 1$.

Applying the parameterization for the 'bounce'

$$\mathrm{i}\theta_{\rm BB}(r) = \left[-\frac{\pi}{2} + \mathrm{i}\phi(r)\right]\mathrm{sign}(y) \qquad \theta_{\rm FF} = \theta_{\rm MF}$$

the first integral takes the form

$$(\nabla_{r/\xi}\phi)^2 + V_{\rm R}(\phi) = V_{\rm R}(\phi_{\rm MF})V_{\rm R}(\phi) = -4\cosh\phi + \kappa^{-1}\cosh 2\phi \tag{17}$$

where $\xi = (D/|y|)^{1/2}$ and

$$\kappa = \tau_n|y|. \tag{18}$$

Here $\phi_{\rm MF} = 0$ for $|y|\tau_n \geqslant 1$, while $\phi_{\rm MF}$ is purely imaginary for $|y|\tau_n < 1$. Typical shapes of the potential $V_{\rm R}(\phi)$ for different values of κ are shown in figure 4. A bounce solution exists only for values of κ bigger than one, while for $\kappa < 1$ the unique solution is the homogeneous one, $\phi = \phi_{\rm MF}$.

For the quasi one-dimensional system, it is possible to derive analytic expressions for both the real instanton action $S_{\rm inst} = 2\pi\nu|y|\xi S_\phi(\kappa)$

$$S_\phi(\kappa) = \int_0^{\phi_{\rm inv}} \mathrm{d}\phi\sqrt{V_{\rm R}(0) - V_{\rm R}(\phi)} \tag{19}$$

where $\phi_{\rm inv} = |\mathrm{arccosh}(2\kappa - 1)|$ is the endpoint of the motion, and the bounce solution $\phi(\boldsymbol{r})$. In particular, for $S_\phi(\kappa)$ we have (figure 6)

$$S_\phi(\kappa) = \sqrt{2\kappa}\left\{-2\frac{\sqrt{\kappa-1}}{\kappa} + 2\arctan\sqrt{\kappa-1}\right\}. \tag{20}$$

At the same time, imposing the boundary conditions $\phi(r \to \pm\infty) = 0$, from the first integral (17) obtains the bounce solution

$$\cosh\phi(r) = \frac{\kappa^2 + 2\mathrm{e}^{-2|r|/r_0(\kappa)}\sqrt{\kappa-1}(3\kappa-2) + \mathrm{e}^{-4|r|/r_0(\kappa)}(\kappa-1)}{\kappa^2 + 2\mathrm{e}^{-2|r|/r_0(\kappa)}\sqrt{\kappa-1}(2-\kappa) + \mathrm{e}^{-4|r|/r_0(\kappa)}(\kappa-1)}$$

where

$$r_0(\kappa) = \left[\frac{D\tau_n}{2(\kappa-1)}\right]^{1/2} \tag{21}$$

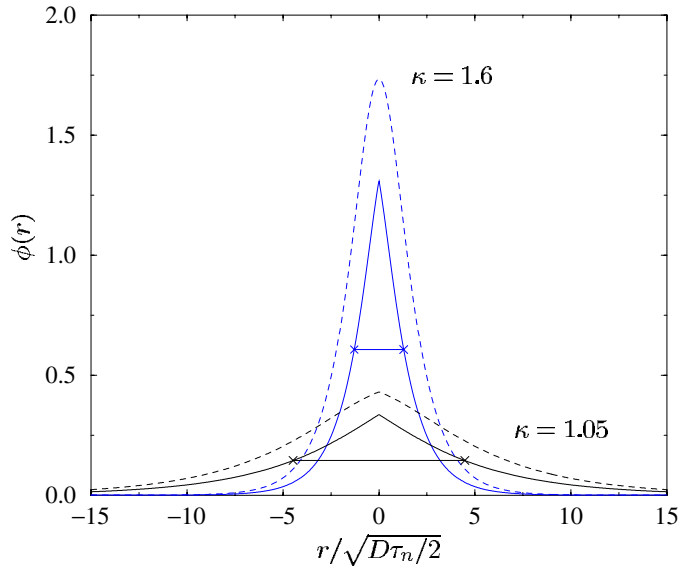

Figure 5. Exact (solid line) and approximate (dashed line) bounce solution $\phi(r)$ versus $r/\sqrt{D\tau_n/2}$ in the quasi one-dimensional geometry for two different values of the inverse of the imaginary 'impurity' concentration, $\kappa = 1.6$ and $\kappa = 1.05$. The interval $[-r_0(\kappa), r_0(\kappa)]$ is explicitly plotted for the exact solutions.

defines the extent of the 'droplet' (see figure 5). In particular, we note that, on approaching the band edge ($\kappa \to 1^+$), $r_0(\kappa) \to \infty$.

Now close to the band edge ($\kappa \to 1^+$), the maximum of the potential $V_R(\phi)$ converges on the two minima allowing the development of a perturbative expansion in $\phi \simeq \phi_{MF} = 0$. Setting $\beta = (4-\kappa)/6\kappa \simeq 1/2$,

$$V_R(\phi) \underset{\phi\simeq 0}{\simeq} V_R(0) - 2\frac{\kappa-1}{\kappa}\phi^2 + \beta\phi^4 + O(\phi^6). \tag{22}$$

In this approximation the action and the bounce solution are given, respectively, by

$$S_\phi(\kappa) \underset{\kappa\gtrsim 1}{\simeq} \frac{4\sqrt{2}}{3}(\kappa-1)^{3/2} \qquad \phi(r) \underset{\kappa\gtrsim 1}{\simeq} 4\sqrt{2}\sqrt{\frac{\kappa-1}{\kappa}}\frac{e^{-|r|/r_0(\kappa)}}{e^{-2|r|/r_0(\kappa)}+4\beta}.$$

This completes the estimate of the contribution to the action from a single bounce configuration. However, to complete the analysis it is necessary to explore the influence of fluctuations around the instanton solution. Here we sketch the important aspects of the analysis referring to details of the parallel discussion by [41] in the context of the disordered superconductor. Generally, field fluctuations around the instanton solution can be separated into 'radial' and 'angular' contributions. The former involve fluctuations of the diagonal elements $\hat{\theta}$, while the latter describe rotations including those Grassmann transformations which mix the BF sector. Both classes of fluctuations play an important role.

Dealing first with the angular fluctuations, supersymmetry breaking of the bounce is accompanied by the appearance of a Grassmann zero-mode separated by an energy gap from higher excitations. This Goldstone mode restores the global supersymmetry of the theory. Crucially, this mode ensures that the saddle-point respects the normalization condition $\langle \mathcal{Z}[0]\rangle_{W,V} = 1$. Associated with radial fluctuations around the bounce, there exists a zero-mode due to translational invariance of the solution, and a negative energy mode (cf [42]).

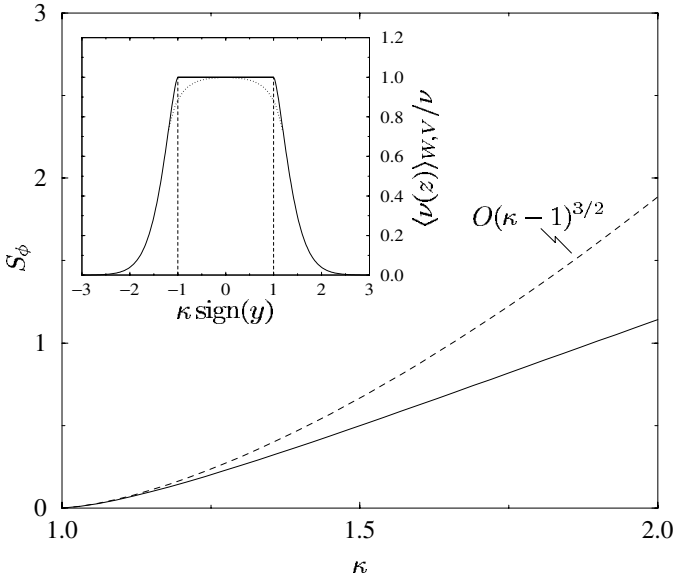

Figure 6. Exact action S_ϕ (solid line) versus κ in the quasi one-dimensional geometry together with the first term of the expansion in $(\kappa - 1)$ (dashed line). The action vanishes as $\kappa \to 1^+$. In the inset, the rescaled DoS $\langle\nu(z)\rangle_{W,V}/\nu \sim \exp[-S_{\rm inst}]$ versus $y\ \tau_n$, for $\pi\nu\sqrt{D/\tau_n} = 2$, is plotted. For values of $\kappa\ \mathrm{sign}(y)$ near the critical values ± 1, the saddle-point analysis becomes unreliable. Here, fluctuations lead to a smooth interpolation between the DoS in the tail region and that comes from the bulk mean-field.

Combining these contributions, one obtains the following expression for the local complex DoS in the tail region,

$$\langle\nu(z,r)\rangle_{W,V} \underset{\kappa>1}{\sim} \mathrm{i}\nu\partial_{z^*}\left[\cosh\phi(r) - \cosh\phi_{\rm MF}\right]|\chi_0(r)|^2\mathrm{e}^{-S_{\rm inst}} \tag{23}$$

where $\chi_0(r)$ represents the eigenfunction for the Grassmann zero mode and $S_{\rm inst}$ denotes the instanton action (20). Thus, to exponential accuracy, the complex local DoS in the tail region becomes non-zero only in the vicinity of the bounce. Mechanisms of quantum interference due to optimal potential fluctuations in the non-Hermitian system conspire to localize states in the tail regions on a length scale $r_0(\kappa)$ greatly in excess of the wavelength $\lambda = 1/k_F$.

2.4.2. Generalization to dimensions $1< d < 4$. Close to the band edge ($\kappa \gtrsim 1$), a generalization of the quasi one-dimensional results to higher dimensions can be developed by dimensional analysis. From the expansion (22) for the potential $V_{\rm R}(\phi)$, the bounce configuration is shown to have the scaling form

$$\phi(\boldsymbol{r}) = \frac{1}{\sqrt{\beta}}\left[\frac{\xi}{r_0(\kappa)}\right] f(\boldsymbol{r}/r_0(\kappa))$$

which, in turn, implies the instanton action (19):

$$S_{\rm inst} \underset{\kappa\gtrsim 1}{\simeq} 4\pi a_d(\Delta\tau_n)^{(d-2)/2} g^{d/2}\left[2(\tau_n|y| - 1)\right]^{(4-d)/2}. \tag{24}$$

Here $g = \nu D L^{d-2}$ and $\Delta = (\nu L^d)^{-1}$ represent, respectively, the dimensionless conductance and average level spacing of the Hermitian system (i.e. with $V = 0$), and a_d is a numerical

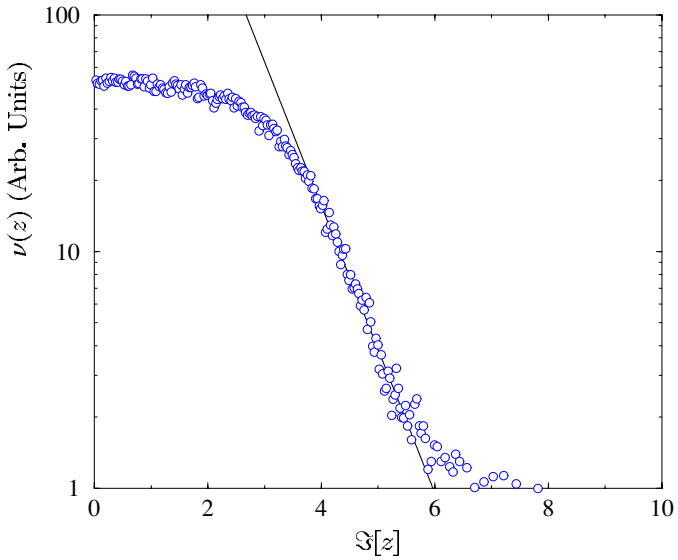

Figure 7. Plot of the (logarithm of the) complex DoS versus $\Im[z] = y$ for a fixed value of $\Re[z] = x$ taken from the numerical simulation of figure 1. The exponential fit of the data is shown as solid curve.

constant ($a_0 = 1/4$ and $a_1 = 1/3$)[4]. Later, in discussing the universality of the results, we will return to consider the zero-dimensional situation.

Taken together with equation (23), this result shows that the complex DoS in the tail region varies exponentially with the separation from the mean-field edge. The power law dependence of the exponent depends on dimensionality, presenting a linear dependence on $(\tau_n|y| - 1)$ in the two-dimensional system. In this case, moreover, the only dependence in (24) on the real part of the energy x occurs through the dimensionless conductance, $g = \nu D \sim |x|$, so that the width of the exponential tail scales as $1/|x|$, as qualitatively appears in figure 1. A comparison with the numerical simulation is shown in figure 7. The results show a good quantitative agreement with the theory for the tail of the DoS. Note that close to (but within) the edge of the support of the spectrum, the saddle-point approximation used in estimating the mean-field DoS becomes unreliable. As shown by the zero-dimensional analysis below, an honest treatment of fluctuations in this region provides a smooth interpolation between the bulk and tail states.

3. Random imaginary vector potential

To conclude our discussion of tail states in the non-Hermitian system, we now turn to an analysis of the random imaginary vector potential Hamiltonian (2). Once again, our approach will be to formulate an effective field theory from which the spectral properties can be determined. Although, as shown in section 2.1, the random vector potential Hamiltonian belongs to a different fundamental symmetry from the random scalar potential Hamiltonian, we show below that, with some qualification, the DoS in the vicinity of the support exhibits the same universal scaling form.

[4] Specifically $a_d = \int d\boldsymbol{u}[(\nabla_{\boldsymbol{u}} f)^2 + f^2(\boldsymbol{u}) - f^4(\boldsymbol{u})]$.

To be concrete, let us consider a d-dimensional Hamiltonian (2) involving an imaginary vector potential field $\boldsymbol{h}(\boldsymbol{r})$ together with a real random scalar potential $W(\boldsymbol{r})$. Once again, let us assume that the scalar potential $W(\boldsymbol{r})$ is drawn from a Gaussian δ-correlated impurity distribution (10). Similarly, we will be primarily concerned with a system exhibiting a random vector potential drawn from a Gaussian distribution with zero mean $\langle \boldsymbol{h}(\boldsymbol{r})\rangle_h = 0$ and correlation

$$\langle h_i(\boldsymbol{q})h_j(\boldsymbol{q}')\rangle_h = (2\pi)^d \delta(\boldsymbol{q}+\boldsymbol{q}') f(|\boldsymbol{q}|)\left[\gamma_1\left(\delta_{ij} - \frac{q_i q_j}{\boldsymbol{q}^2}\right) + \gamma_2 \frac{q_i q_j}{\boldsymbol{q}^2}\right]. \quad (25)$$

Here, for reasons that will become clear below, we have introduced an 'envelope' $f(|\boldsymbol{q}|)$ which limits the correlations of the fields at both microscopic and macroscopic length scales. Setting

$$\boldsymbol{h}(\boldsymbol{r}) = \nabla\varphi(\boldsymbol{r}) + \nabla \wedge \boldsymbol{\chi}(\boldsymbol{r}) \quad (26)$$

γ_1 is identified as the strength of fluctuations of the incompressible component of the vector field, $\boldsymbol{\chi}(\boldsymbol{r})$, while γ_2 controls the irrotational part, $\varphi(\boldsymbol{r})$. In the following, it will also be useful to contrast the behaviour of the random vector potential system with that of a *constant* vector field $\boldsymbol{h}(\boldsymbol{r}) = \text{const} = \boldsymbol{h}_0$—the Hatano–Nelson system [3].

3.1. Background

Before turning to the formal analysis of the statistical field theory, that begins with some general considerations which identify certain idiosyncrasies of the constant vector potential system and how they impact upon the existence of tail states in the random vector potential system. Previous investigations of the former have revealed unusual localization properties of the random Hamiltonian which contrast with those of its Hermitian (i.e. $\boldsymbol{h}_0 = 0$) counterpart. Specifically, it was shown in [3] that, for the strictly one-dimensional system subject to *periodic boundary conditions* at infinity, when the field, $|\boldsymbol{h}_0|$, exceeds a critical value h_c corresponding to the (energy dependent) localization length $\xi_{\text{loc}} = 1/h_c$ of the Hermitian system, there is a transition to a delocalized phase. Since then, this result has been generalized to the quasi-one-dimensional system by Kolesnikov and Efetov [18] using techniques which parallel those discussed here.

Now, following [3], a simple argument can be established to describe qualitatively the origin of the transition. For a constant imaginary vector potential, $\boldsymbol{h}_0$, a similarity transformation of the left and right eigenfunctions $\phi_i^L(\boldsymbol{r}) \mapsto \phi_i^L(\boldsymbol{r})\exp(-\boldsymbol{h}_0 \cdot \boldsymbol{r})$ and $\phi_i^R(\boldsymbol{r}) \mapsto \exp(\boldsymbol{h}_0 \cdot \boldsymbol{r})\phi_i^R(\boldsymbol{r})$ removes its dependence on $\boldsymbol{h}_0$ from the Hamiltonian. Being now Hermitian, the eigenvalues of the Hamiltonian must, therefore, be real and specified by those of the unperturbed random system. However, if periodic boundary conditions are imposed, the similarity transformation must be applied with caution: if the eigenfunctions of the Hermitian system are localized on a length scale $\xi_{\text{loc}} < |\boldsymbol{h}_0|$ the similarity transformation is incompatible with the periodic boundary conditions and cannot be imposed. Here there is a transition from a localized phase, where the eigenvalues are real, to a delocalized phase where the eigenvalues migrate into the complex plane.

Now what does this phenomenology tell us about the existence of the tail states? Using the same arguments, it is easy to deduce that optimal fluctuations of the impurity potential can *not* induce localized tail states in the constant vector potential system: suppose that a tail state appeared at some complex energy outside the band of bulk states. If the state is localized, it must be insensitive to the boundary conditions at infinity and, therefore, its dependence on the constant field can be removed by a similarity transformation. As such, it must therefore be contained within the Hermitian theory, and its eigenvalue must be real. This contradiction

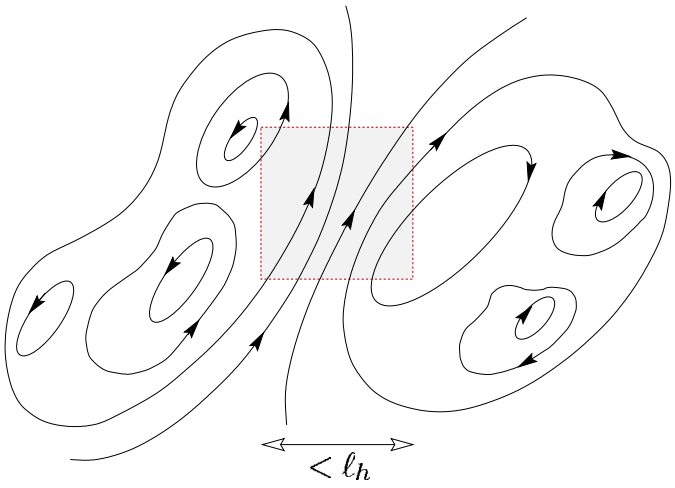

Figure 8. A typical field configuration of the random vector field. Over the interval ℓ_h, the flux lines of $\boldsymbol{h}$ are approximately constant, preventing the existence of tail state.

strictly eliminates tail states from the infinite constant imaginary vector potential system. (Of course, the Hermitian system can and will exhibit low-energy Lifshitz band tail states.)

With this background, let us now turn to consider the random vector potential system. Once again, for a random field $\boldsymbol{h}(\boldsymbol{r})$ drawn from the Gaussian distribution (25), it is straightforward to confirm that the similarity transformation $\phi_i^L(\boldsymbol{r}) \mapsto \phi_i^L(\boldsymbol{r}) \exp[-\varphi(\boldsymbol{r})]$ and $\phi_i^R(\boldsymbol{r}) \mapsto \exp[\varphi(\boldsymbol{r})]\phi_i^R(\boldsymbol{r})$ remove the dependence on the incompressible component, $\varphi(\boldsymbol{r})$ from the Hamiltonian. Therefore, when subject to any *purely* irrotational vector field $\boldsymbol{h}(\boldsymbol{r}) = \nabla\varphi(\boldsymbol{r})$ (with zero average), the eigenvalues remain real and coincide with those of the Hermitian system. Conversely, the incompressible field distribution $\boldsymbol{h}(\boldsymbol{r}) = \nabla \wedge \boldsymbol{\chi}(\boldsymbol{r})$ cannot be removed by similarity transformation. Such field configurations necessarily generate states with complex eigenvalues.

Now, the random distribution (25) with $f(|\boldsymbol{q}|) = 1$ imposes long-ranged, i.e. power-law correlations in the incompressible field configuration. As well as admitting superdiffusion processes [43–45] which dominate the relaxation to equilibrium in the classical system, these long-range correlations impact upon the probability of finding tail states in the non-Hermitian system: any random configuration of the incompressible field will involve field lines correlated over arbitrarily long distances. These field lines advect particles in the classical system and are responsible for the characteristic superdiffusion properties of the system. Now in such a background, one can identify regions where the field lines are oriented over long distances, say ℓ_h (see figure 8). Within this region, the nucleation of tail states with a localization length $r_0 < \ell_h$ is prohibited by the same mechanism described above for the Hatano–Nelson system. Clearly, the phenomenology of tail state formation in the superdiffusive system is subtle, being sensitive to the arrangement of both the scalar *and* the vector field.

Therefore, since we are interested here in exposing the general principles behind tail state formation in the non-Hermitian system, to keep our discussion simple, we will limit our considerations to distributions where the correlations of the field lines are limited to a length scale ℓ_h much smaller than the localization length of the incipient tail states, r_0, i.e. introducing a microscopic cut-off a, we set

$$f(|q|) = \begin{cases} 1 & 1/\ell_h < |\boldsymbol{q}| < 1/a \\ 0 & \text{otherwise} \end{cases}$$

where ℓ_h represents the maximum length scale of the field correlations. With these considerations in mind, let us now turn to the development of the field theory of the non-Hermitian system.

3.2. Field theory

Following the method outlined for the imaginary scalar potential system, our starting point is the gauge-transformed 'Hermitized' matrix Hamiltonian (6). Now, under the 'charge-conjugation' operation, the Hamiltonian transforms as

$$\sigma_2 \left[\hat{\mathcal{H}}_\Gamma(\boldsymbol{h})\right]^{\mathsf{T}} \sigma_2 = -\hat{\mathcal{H}}_\Gamma(-\boldsymbol{h}).$$

The statistical properties of the non-Hermitian system can again be obtained from the generating function (8) by forming an average over the real random potential $W(\boldsymbol{r})$ and introducing a slow-field decoupling. In doing so, one obtains the generating functional

$$\langle \mathcal{Z}[0] \rangle_W = \int DQ \exp\left[\frac{\pi\nu}{8\tau}\int \mathrm{d}\boldsymbol{r}\ \mathrm{str}\, Q^2 - \frac{1}{2}\int \mathrm{d}\boldsymbol{r}\ \mathrm{str}\langle \boldsymbol{r}|\ln \hat{\mathcal{G}}^{-1}|\boldsymbol{r}\rangle\right] \tag{27}$$

where

$$\hat{\mathcal{G}}^{-1} = \mathrm{i}\eta\sigma_3 \otimes \sigma_3^{\mathrm{CC}} + x - \frac{1}{2m}\left[\hat{\boldsymbol{p}} - \mathrm{i}\boldsymbol{h}(\boldsymbol{r})\sigma_1 \otimes \sigma_3^{\mathrm{CC}}\right]^2 - \mathrm{i}y\sigma_1 + \frac{i}{2\tau}Q(\boldsymbol{r})$$

denotes the supermatrix Green function. As with the scalar potential, further progress is possible only within a saddle-point approximation. However, following our discussion above, it is now necessary to exercise some caution.

In the Hermitian system with a real vector potential $\boldsymbol{A} = \mathrm{i}\boldsymbol{h}$, the conventional approach [35] involves subjecting the action to a saddle-point approximation in the absence of the field. The saddle-point manifold $Q^2 = \mathbb{I}$ is unperturbed by the real vector potential and its effect on the low-energy properties of the system can be accommodated at the level of the gradient expansion. However, as emphasized in [18], in the presence of a *constant* imaginary vector potential, $\boldsymbol{h}(\boldsymbol{r}) = \boldsymbol{h}_0$, depending on the magnitude of $\boldsymbol{h}_0$, it is possible to identify separate saddle-points of the total effective action (27). Inside the localized phase (i.e. $|\boldsymbol{h}_0| < h_c$), the dependence on $\boldsymbol{h}_0$ can (and must) be removed by a rotation of Q—the counterpart of the similarity transformation. The resulting theory reflects that of the Hermitian model and the eigenvalues condense onto the real line. Conversely, in the delocalized phase (i.e. $|\boldsymbol{h}_0|\rangle h_c$), the similarity transformation on Q is inadmissible. Here the dependence of the action on $\boldsymbol{h}_0$ must be developed explicitly, reflecting the fact that the eigenvalues acquire an imaginary component. Similarly, for a random vector potential, it is necessary to remove the irrotational component of the field $\boldsymbol{h}$ (i.e. $\nabla\varphi(\boldsymbol{r})$) explicitly at the level of the saddle-point by subjecting Q to a similarity transformation

$$Q(\boldsymbol{r}) \mapsto \mathrm{e}^{-\varphi(\boldsymbol{r})\sigma_1\otimes\sigma_3^{\mathrm{CC}}} Q(\boldsymbol{r}) \mathrm{e}^{\varphi(\boldsymbol{r})\sigma_1\otimes\sigma_3^{\mathrm{CC}}}.$$

As expected, the same transformation leaves the source term for the DoS (15) unperturbed.

Without the irrotational component of the field, the saddle-point of the total action can be analysed in the usual way, following a two-stage procedure. As before, taking into account the quasi-classical parameter $x\tau \gg 1$, one finds that the low-energy fluctuations are confined to the manifold $Q^2(\boldsymbol{r}) = \mathbb{I}$. Then, subjecting the action to a gradient expansion keeping $y\tau \ll 1$ and $\sqrt{\gamma_1} \ll \ell^{-1}$, one obtains the non-linear σ-model action [4, 18, 35]

$$S[Q] = -\frac{\pi\nu}{8}\int \mathrm{d}\boldsymbol{r}\ \mathrm{str}\left[D(\widetilde{\nabla}Q)^2 - 4\left(\eta\sigma_3 \otimes \sigma_3^{\mathrm{CC}} - y\sigma_1\right)Q\right] \tag{28}$$

where $\widetilde{\nabla} = \nabla - \boldsymbol{h}\left[\sigma_1 \otimes \sigma_3^{\mathrm{CC}}\right]$ represents the covariant derivative, and $\boldsymbol{h} \equiv \nabla \wedge \boldsymbol{\chi}$ reflects the incompressible component of the field.

Now, although the structure of the action compares with that of the imaginary scalar potential field, it exhibits important differences which substantially influence the behaviour of the system: specifically, in addition to the 'diamagnetic' contribution, i.e. the term proportional to $\boldsymbol{h}^2$, the action presents a paramagnetic contribution, linear in $\boldsymbol{h}$, which couples with the gradient of Q. Although this term does not affect the homogeneous saddle-point solution, it is responsible for the destabilisation of the tail states in the system with long-range correlations. To see this explicitly, let us return to the consideration of the constant vector potential system. Previously, in the qualitative discussion above, it was argued that such a system does not accommodate tail states. How is this phenomenon reflected in the field theory?

In fact, for $\boldsymbol{h}(\boldsymbol{r}) = \boldsymbol{h}_0 > h_c$, the action is still given by the non-linear σ-model (28). However, in view of the paramagnetic term, to explore the saddle-point structure, it is necessary to adopt a more general parameterization, $Q = \sigma_1 \cos\hat{\theta} + \sin\hat{\theta} e^{\hat{\rho}\sigma_1 \otimes \sigma_3^{CC}} \sigma_3 \otimes \sigma_3^{CC}$, where $\hat{\rho} = \mathrm{diag}(\rho_{BB}, \rho_{FF})_{B,F}$. In doing so, two coupled equations for $\hat{\theta}$ and $\hat{\rho}$ are obtained:

$$D\nabla^2\hat{\theta} + \frac{D}{2}\sin 2\hat{\theta}\left[(\nabla\hat{\rho})^2 + 4|\boldsymbol{h}_0|^2 + 4\boldsymbol{h}_0 \cdot \nabla\hat{\rho}\right] + 2y\sin\hat{\theta} = 0$$
$$\nabla \cdot \left[\sin^2\hat{\theta}\,(\nabla\hat{\rho} + 2\boldsymbol{h}_0)\right] = 0. \tag{29}$$

To understand the nature of these equations, let us focus on the quasi-one-dimensional system. In this case the second equation can be integrated and substituted in the first one, giving, respectively

$$D\nabla^2\hat{\theta} + D\boldsymbol{j}^2\frac{\cos\hat{\theta}}{\sin^3\hat{\theta}} + 2y\sin\hat{\theta} = 0 \qquad \nabla\hat{\rho} = -2h_0 + \frac{\boldsymbol{j}}{\sin^2\hat{\theta}}$$

where $\boldsymbol{j}$ is a constant fixed by the boundary conditions. From these equations one can identify a homogeneous supersymmetric solution, $\nabla\hat{\rho} = 0$ and

$$\cos\theta_{MF} = \begin{cases} -y\tau_n & |y|\tau_n < 1 \\ -\mathrm{sign}(y) & |y|\tau_n \geqslant 1 \end{cases} \tag{30}$$

where $1/\tau_n = 2D|\boldsymbol{h}_0|^2$. Again, making use of equation (7), the homogeneous solution translates to a complex DoS (16), which is flat and non-vanishing only in the interval $|y|\tau_n > 1$. Now, in the imaginary scalar potential problem, an instanton configuration of the saddle-point equation was signalled by the existence of tail states. What happens in the present case? Since, at infinity, the instanton solution is constrained to be the homogeneous one, the constant $\boldsymbol{j}$ is determined by the homogeneous mean-field solution, $\boldsymbol{j} = 2\boldsymbol{h}_0 \sin^2\theta_{MF}$. Therefore, using (30) one can see that outside the bulk of the spectral support $\boldsymbol{j}$ vanishes. Therefore, the equation of motion for $\hat{\theta}$ does not admit the existence of an instanton. As expected from the qualitative discussion above, tails are therefore excluded from the constant imaginary vector potential problem.

Similarly, in the random vector potential system with long-ranged correlations (i.e. for $f(|\boldsymbol{q}|) = 1$), we can expect the paramagnetic term to present a similar role. Indeed, subjecting the generating functional to an average over the random distribution (25), one obtains a non-local interaction of the fields. In the present context, such terms have been shown by Taras-Semchuk and Efetov [46] to reproduce the known renormalization properties of the superdiffusive system. However, in the present case, we have limited our considerations to correlations of the vector field which extend over a maximum range ℓ_h. Then, taking the relevant field configurations of Q (i.e. those involving the instanton solution) to be long-ranged on a scale r_0 greatly in excess of ℓ_h, the vector field entering the paramagnetic term can be

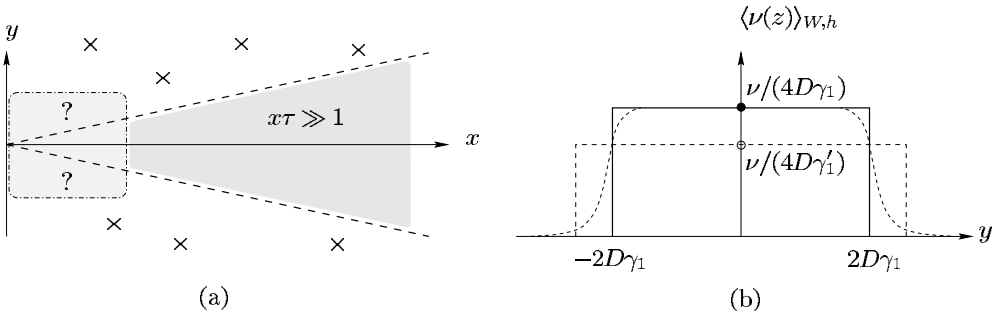

Figure 9. Complex DoS for the imaginary vector potential problem in the quasi-classical limit $x\tau \gg 1$ for the two-dimensional system. (*a*) In the mean-field approximation, the DoS is equal to $\nu/(4D\gamma_1)$ inside the region $|y| \leqslant 2D\gamma_1 = 2\tau\gamma_1|x|/m$ of the complex plane $z = x + \mathrm{i}y$ and zero otherwise; (*b*) $\langle \nu(z) \rangle_{W,h}$ versus y for two values of $\gamma_1 < \gamma_1'$. The tails of the DoS for $|y| \rangle 2\tau\gamma_1|x|/m$ are shown schematically.

replaced by its spatial average, i.e. the paramagnetic term can be eliminated. By contrast, the diamagnetic contribution survives spatial averaging. The total action assumes the form

$$S[Q] = -\frac{\pi\nu}{8}\int \mathrm{d}\boldsymbol{r}\ \mathrm{str}\left[D(\nabla Q)^2 - 4\big(\eta\sigma_3 \otimes \sigma_3^{\mathrm{CC}} - y\sigma_1\big)Q + \frac{1}{\tau_n}\big(Q\sigma_1 \otimes \sigma_3^{\mathrm{CC}}\big)^2\right] \tag{31}$$

where, setting $\tilde{\gamma}_1 = \gamma_1 L^d \int \mathrm{d}\boldsymbol{q}/(2\pi)^d\ f(|\boldsymbol{q}|)$

$$\frac{1}{\tau_n} = 2(d-1)D\tilde{\gamma}_1.$$

Now, as with the imaginary scalar potential, the profile of the bulk DoS and tail states can be obtained by subjecting the action to a saddle-point analysis. Varying the action with respect to Q, subject to the non-linear constraint $Q^2 = \mathbb{I}$, one obtains the homogeneous saddle-point equation,

$$D\nabla(Q\nabla Q) - \big[\eta\sigma_3 \otimes \sigma_3^{\mathrm{CC}} - y\sigma_1,\, Q\big] + \frac{1}{2\tau_n}\big[\sigma_1 \otimes \sigma_3^{\mathrm{CC}} Q \sigma_1 \otimes \sigma_3^{\mathrm{CC}},\, Q\big] = 0.$$

Then, applying the ansatz $Q = \cos\hat{\theta}\sigma_3 \otimes \sigma_3^{\mathrm{CC}} + \sin\hat{\theta}\sigma_1$, where $\hat{\theta} = \mathrm{diag}(\mathrm{i}\theta_{\mathrm{BB}}, \theta_{\mathrm{FF}})_{\mathrm{B,F}}$, the saddle-point equation coincides with equation (13) allowing the results of sections 2.3 and 2.4.2 to be imported. As a result, we can immediately deduce the homogeneous mean-field solution (14) as well as the inhomogeneous instanton solution (13) of the saddle-point equation. Thus, from the homogeneous mean-field solution, one obtains the expression (16) for the DoS, i.e. the complex DoS is flat and non-vanishing over the interval

$$|y| < \frac{1}{\tau_n} = \frac{4(d-1)}{d}\frac{\tilde{\gamma}_1|\tau}{m}|x|.$$

i.e., in the two-dimensional system, the support for the DoS occupies a wedge of the complex plane with a width that scales in proportion to $\tilde{\gamma}_1|x|$ (see figure 9). Furthermore, making use of equations (23) and (24), one obtains complex DoS in the tail region,

$$\langle \nu(z) \rangle_{W,h} \sim \exp\big\{-4\pi a_d(\Delta\tau_n)^{(d-2)/2} g^{d/2}\,[2(\tau_n|y| - 1)]^{(4-d)/2}\big\}$$

where, as usual, $g = \nu D L^{d-2}$ and $\Delta = (\nu L^d)^{-1}$ represent, respectively, the dimensionless conductance and average level spacing of the Hermitian system.

In fact, the behaviour of the vector potential system differs from the scalar potential system only in the symmetry of the soft fluctuations around the saddle-point solution. As

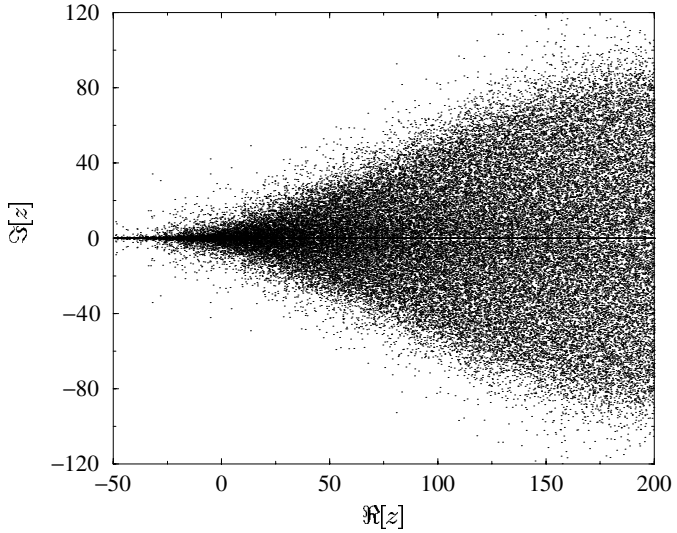

Figure 10. Complex eigenvalues for several realizations of the non-Hermitian vector potential Hamiltonian, where the potential W is drawn from a Gaussian δ-correlated random impurity distribution. Here we have included a lattice of 29×29 $\boldsymbol{q}$-points in the momentum space. Note that the constraints on the numerical simulation limit the relevant data to the interval $x = \Re[z] < 200$.

usual, the homogeneous saddle-point solution Q_{MF} is not unique but is spanned by an entire manifold of solutions $Q = TQ_{\mathrm{MF}}T^{-1}$ where for $y \neq 0$, $[T, \sigma_1] = 0 = \left[T, \sigma_1 \otimes \sigma_3^{\mathrm{CC}}\right]$ with $T = \gamma(T^{-1})^{\mathsf{T}}\gamma^{\mathsf{T}}$ (chiral symmetry class AIII in the classification [36]), while, for $y = 0$, $\left[T, \sigma_1 \otimes \sigma_3^{\mathrm{CC}}\right] = 0$ (chiral symmetry class BDI). Now while the soft (class AIII) fluctuations decouple from the DoS source (cf the scalar potential Hamiltonian), the soft (class BDI) fluctuations couple. As a result, the complex DoS becomes strongly suppressed near $y = 0$, while on the real axis, a finite density of eigenvalues accumulates as shown below.

The amalgamation of data for the eigenvalues of ca 100 realizations of the imaginary vector potential Hamiltonian is shown in figure 10. The locus of the edge of the support predicted by the mean-field theory is in good agreement with the numericals, while the depletion of eigenvalues from the interval near $y = 0$ and the singular density at $y = 0$ are clearly resolved. In particular, a comparison of the complex DoS with the numerical simulation shown in figure 11 gives a good agreement with the theory.

3.3. Zero-dimensional limit

Finally, to conclude our discussion, let us turn to consider the properties of the imaginary vector potential Hamiltonian when the system enters the zero-dimensional limit. Our analysis above shows that, outside the region of support, the spectrum is characterized by tail states which are localized on a length scale of $r_0(\kappa)$ as given in (21). When the size of the droplet region becomes in excess of the system size (inevitable in a finite system as one approaches the edge of the support, $\kappa \to 1^+$), the system enters a zero-dimensional regime where the action is dominated by the zero spatial mode of Q. Here the action collapses onto the zero-dimensional theory analysed in detail by Efetov [4].

In this limit, we can proceed in two ways: firstly, following the discussion above, we can apply the saddle-point analysis seeking a symmetry-broken field configuration. However, in this case, the relative of the bounce solution is now a stationary point of the zero-dimensional

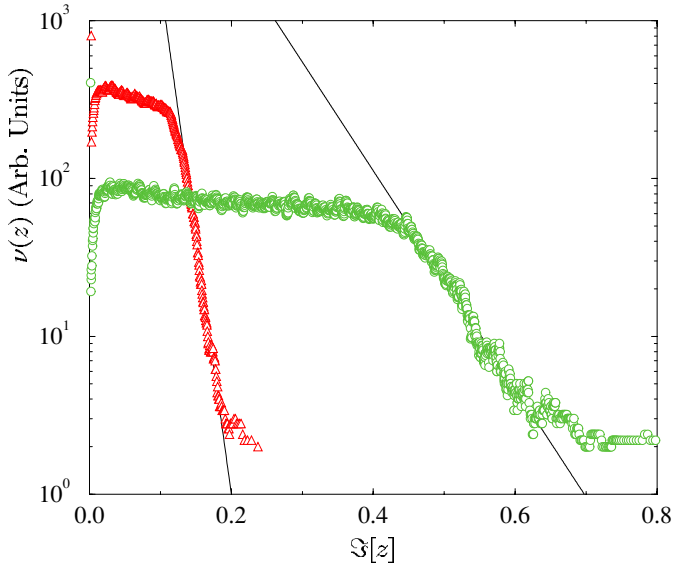

Figure 11. Logarithm of the complex DoS versus $\Im[z] = y$ for a fixed value of $\Re[z] = x$ taken from the numerical simulation of figure 10 (triangles). A second data set (circles) is shown for a value of $\tilde{\gamma}_1$ four times as large. Note that, as expected from the theory, the change in $\tilde{\gamma}_1$ is reflected in the slope of the exponent. The exponential fits of the two data are shown as solid curves.

potential $V(\phi)$. Alternatively, following Efetov [4] one can undertake an exact evaluation of the zero-dimensional σ-model. A pursuit of the second route obtains the exact formula for the complex DoS. The latter can be separated into two contributions $\nu(z) = \nu_r(z) + \nu_c(z)$,where

$$\nu_r(x, y) = \nu\delta(y)\int_0^1 \mathrm{d}t\, \mathrm{e}^{-a^2t^2} \qquad \nu_c(x, y) = \frac{\pi\nu}{\Delta}\Phi\left(\frac{\chi}{2a}\right)\int_0^1 \mathrm{d}t\; t\sinh(\chi t)\,\mathrm{e}^{-a^2t^2}$$

where

$$\chi = \frac{2\pi|y|}{\Delta} \qquad a^2 = \frac{\pi}{\Delta\tau_n}$$

with $\Phi(u) = 2\int_u^\infty \mathrm{d}t\ \mathrm{e}^{-t^2}/\sqrt{\pi}$ and Δ is the level spacing of the Hermitian system. The presence of the anomalous part $\nu_r(x, y)$ attests that a finite fraction of the eigenvalues remains real. Otherwise the component $\nu_c(x, y)$ describes the distribution of complex eigenvalues and its form is shown in figure 12. In the region $\chi \gg 2a$ the DoS coincides with the constant mean-field value (16) for $\chi > 2a^2$, while outside this interval one has the following asymptotic expansion:

$$\nu_c(x, y) \underset{\chi>2a^2}{\simeq} \frac{\sqrt{\pi}\nu}{\Delta}\frac{a}{\chi^2}\exp\left(\chi - \frac{\chi^2}{4a^2} - a^2\right). \tag{32}$$

With the exact result at hand, let us compare equation (32) with the result of the saddle-point analysis from the symmetry-broken field configuration. In particular, in the zero-dimensional case, the saddle-point analysis leads to the 'instanton' action

$$S_{\mathrm{inst}} = \frac{\pi|y|}{2\Delta}[V_{\mathrm{R}}(0) - V_{\mathrm{R}}(\phi_{\mathrm{min}})]$$

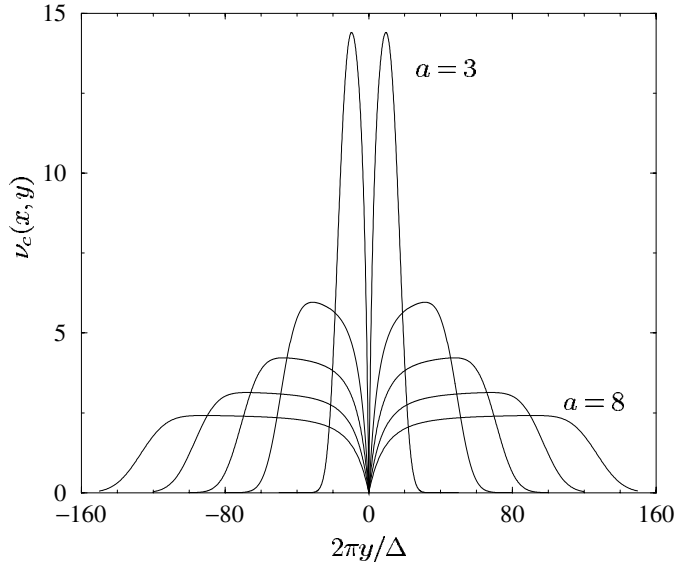

Figure 12. Complex DoS $\nu_c(z)$ as a function of $2\pi y/\Delta$ for $\nu = 10$ and $a = 3, 5, 6, 7, 8$.

where $\phi_{\min}$ is the minimum of the potential $V_R(\phi)$ (figure 4). Evaluating this minimum, one obtains

$$S_{\text{inst}} = \frac{\pi}{\Delta\tau_n}(|y|\tau_n - 1)^2 = \frac{\chi^2}{4a^2} - \chi + a^2.$$

From the expression for the DoS (23), we can conclude that, in the zero-dimensional case, the exponential dependence of the DoS coincides with the exact result obtained in [4].

4. Conclusions

To conclude, we have implemented a field theoretic scheme to explore the structure of the DoS close to the edge of the support of two linear non-Hermitian operators describing a quantum particle subject to a random imaginary scalar and an imaginary vector potential. In doing so, we have provided a general scheme for the symmetry classification of non-Hermitian operators. The field theoretic approach is easily generalized for the consideration of higher point spectral correlations of the fields.

In the quasi-classical limit, where the real part of the energy is in excess of any other energy-scale, the tails are dominated by 'optimal configurations' of the real random scalar potential. In contrast to band tail states in semi-conductors, these states are quasi-classical in nature being localized on the length scale $\xi = (D/|y|)^{1/2} \gg \ell$. As such the profile of the DoS and their dimension is universal depending on just a few material parameters and independent of the nature of the impurity distribution. In the particular case of the constant imaginary vector potential, we have argued that tail states of the system are prohibited by the delocalization mechanism of Hatano and Nelson.

Acknowledgments

We are grateful to Victor Gurarie and Damian Taras-Semchuk for useful discussions. One of us (FMM) would like to acknowledge the financial support of Scuola Normale Superiore.

References

[1] Sommers H J, Crisanti A, Sampolinski H and Stein Y 1988 *Phys. Rev. Lett.* **60** 1895
[2] Haake F, Izrailev F, Lehmann N, Saher D and Sommers H -J 1992 *Z. Phys.* B **88** 359
[3] Hatano N and Nelson D R 1996 *Phys. Rev. Lett.* **77** 570
Hatano N and Nelson D R 1997 *Phys. Rev.* B **56** 8651
[4] Efetov K B 1997 *Phys. Rev.* B **56** 9630
Efetov K B 1997 *Phys. Rev. Lett* **79** 491
[5] Brouwer P W, Silvestrov P G and Beenakker C W J 1997 *Phys. Rev.* B **56** R4333
[6] Fyodorov Y V, Khoruzhenko B A and Sommers H -J 1997 *Phys. Lett.* A **226** 46
Fyodorov Y V, Khoruzhenko B A and Sommers H -J 1997 *Phys. Rev. Lett.* **79** 557
[7] Janik R A, Nowak M A, Papp G and Zahed I 1997 *Nucl. Phys* B **501** 603
[8] Feinberg J and Zee A 1997 *Nucl. Phys.* **504** 579
[9] Chalker J T and Wang Z J 1997 *Phys. Rev. Lett.* **79** 1797
[10] Brézin E and Zee A 1998 *Nucl. Phys.* B **509** 599
Feinberg J and Zee A 1999 *Phys. Rev.* E **59** 6433
[11] Mudry C, Simons B D and Altland A 1998 *Phys. Rev. Lett.* **80** 4257
[12] Chalker J T and Mehlig B 1998 *Phys. Rev. Lett.* **81** 3367
Mehlig B and Chalker J T *preprint* cond-mat/9906279
[13] Hastings M B 2001 *J. Stat. Phys.* **103** 903
[14] Janik R A, Noerenberg W, Nowak M A, Papp G and Zahed I 1999 *Phys. Rev.* E **60** 2699
[15] Izyumov A V and Simons B D 1999 *Europhys. Lett.* **45** 290
[16] Izyumov A V and Simons B D 1999 *Phys. Rev. Lett.* **83** 4373
[17] Yurkevich I V and Lerner I V 1999 *Phys. Rev. Lett.* **82** 5080
[18] Kolesnikov A V and Efetov K B 2000 *Phys. Rev. Lett.* **84** 5600
[19] Mudry C , Brouwer P W, Halperin B I, Gurarie V and Zee A 1998 *Phys. Rev.* B **58** 13539
[20] Edwards S F 1965 *Proc. Phys. Soc.* **85** 613
[21] Kleinert H 1995 *Path Integrals in Quantum Mechanics, Statistics and Polymer Physics* (Singapore: World Scientific)
[22] Bouchaud J P and Georges A 1990 *Phys. Rep.* **195** 127
[23] Isichenko M B 1992 *Rev. Mod. Phys.* **64** 961
[24] Abrahams E, Anderson P W, Licciardello D C and Ramakrishnan T V 1979 *Phys. Rev. Lett.* **42** 673
[25] Gor'kov L P, A I Larkin and Khmel'nitskii D E 1979 *JETP Lett.* **30** 228
[26] Ginibre J 1965 *J. Math. Phys.* **6** 440
[27] Gir'ko V L 1985 *Theor. Prob. Appl.* **29** 694
[28] Balagurov Ya B and Vaks V G 1974 *Sov. Phys. JETP* **38** 968
[29] Samokhin K 1998 *J. Phys. A : Math. Gen.* **31** 9455
[30] Shnerb N M 1998 *Phys. Rev.* B **57** 8571
[31] Lifshitz I M 1965 *Sov. Phys. Usp.* **7** 549
Lifshitz I M 1964 *Adv. Phys.* **13** 483
Lifshitz I M 1967 *Zh. Eksp. Teor. Fiz.* **53** 743
[32] Zittartz J and Langer J S 1966 *Phys.Rev.* **148** 741
[33] Halperin B I and Lax M 1966 *Phys. Rev.* **148** 722
[34] Lifshitz I M, Gredeskul S A and Pastur L A 1976 *Sov. J. Low Temp. Phys.* **2** 533
[35] Efetov K B 1997 *Supersymmetry in Disorder and Chaos* (Cambridge: Cambridge University Press)
[36] Zirnbauer M R 1996 *J. Math. Phys.* **37** 4986
[37] Altland A, Simons B D and Taras-Semchuk J P D 1998 *Adv. Phys.* **49** 321
[38] Bundschuh R, Cassanello C, Serban D and Zirnbauer M R 1998 *Nucl. Phys.* B **532** 689
[39] Simons B D and Altland A 2000 Mesoscopic Physics *Proc. CRM Summer School Theoretical Physics at the End of the XXth Century (Banff, Canada 1999) (CRM Series in Mathematical Physics)* (Berlin: Springer)
[40] Abrikosov A A and Gor'kov L P 1961 *Sov. Phys. JETP* **12** 1243
[41] Lamacraft A and Simons B D 2000 *Phys. Rev. Lett.* **85** 4783
Lamacraft A and Simons B D 2001 *Preprint* cond-mat/0101080
[42] Coleman S 1985 *Aspects of Symmetry. Selected Erice lecture* (Cambridge: Cambridge University Press)
[43] Derrida B and Luck J M 1983 *Phys. Rev.* B **28** 7183
[44] Kravtsov V E, I V Lerner and Yudson V I 1986 *Sov. Phys. JETP* **64** 336
[45] Fisher D S 1984 *Phys. Rev.* A **30** 960
[46] Taras-Semchuk D and Efetov K B 2001 *Phys. Rev.* B **64** 115301